ELSEVIER

Polymer 43 (2002) 6973–6983

polymer

www.elsevier.com/locate/polymer

Free volume and glass transition in ethylene/1-octene copolymers: positron lifetime studies and dynamic mechanical analysis

D. Kilburn[a], D. Bamford[a], T. Lüpke[b], G. Dlubek[a,c,*], T.J. Menke[b], M.A. Alam[a]

[a]*H.H. Wills Physics Laboratory, University of Bristol, Tyndall Avenue, Bristol BS8 1 TL, UK*
[b]*Martin-Luther-Universität Halle-Wittenberg, Fachbereich Ingenieurwissenschaften, D-06099 Halle/S, Germany*
[c]*ITA Institut für innovative Technologien GmbH, Köthen, Aussenstelle Halle, Wiesenring 4, Lieskau (bei Halle/S) D-06120, Germany*

Abstract

Semicrystalline ethylene/1-octene copolymers (P(E-*co*-O)) with a content of 1-octene comonomer, w_O, between 7 and 24 wt% and a crystallinity X_c between 50 and 10% and a high-density polyethylene (HDPE, $X_c = 70\%$) were studied in the temperature range between 115 K and (300–350) K by positron annihilation lifetime spectroscopy (PALS) and dynamic mechanical analysis (DMA). The samples were characterised by differential scanning calorimetry (DSC) and wide-angle X-ray scattering (WAXS). The T_gs estimated from the thermal expansion of the local free volume estimated from the PALS data decrease linearly with w_O between 251 K (extrapolated to $w_O = 0$) and 220 K ($w_O = 24$ wt%). They agree very well with those estimated from DMA (loss modulus E'') and DSC. However, the T_gs obtained from the maximum of tan δ do not agree with all of the others, inparticular for higher crystallinities. For HDPE, any indication of a glass transition could not be observed. From this it was concluded that the whole amorphous phase in this highly crystalline polymer is immobile. From the variation of the thermal expansivity of the local free volume the fractions of the mobile and immobile amorphous phase are estimated. It was observed that the *o*-Ps intensity shows a minimum at $T_{min} \approx T_g + 10$ K.

Keywords: Ethylene–octene copolymers; Glass transition; Free volume

1. Introduction

In recent years, the application of positron annihilation lifetime spectroscopy [1,2] (PALS) in the studies of polymer properties has seen a remarkable increase [3,4]. PALS provides unique information about the properties of subnanometer local free volumes (holes) which appear in amorphous polymers [5–11] due the structural disorder. These holes form the (excess) free volume which effects thermal, mechanical and relaxation properties of polymers. It lowers the density of the amorphous polymer by about 10% compared with the crystalline state of the same material. The transport of small molecules, such as gases and water, occurs via these holes. Therefore, close relations between the segmental mobility and the free volume are expected [12–14] and also observed [15–17].

During the glass transition, the structural disorder within a polymer changes its character from a static to a dynamic one with increasing segmental motions that result in a distinct increase of the hole sizes with increasing temperature. In a material with well defined glass transition temperature (T_g), PALS data reveals an abrupt increase in the slope of the thermal expansion of the hole volumes as a function of temperature at T_g. This temperature is usually determined from the intersection of two straight lines asymptotically fitted to the free volume expansion curves in the temperature ranges, below and above, close to the expected T_g.

In amorphous polymers, T_g values derived from PALS agree within their error limits with those from pressure–volume–temperature (PVT) experiments [18] when different heating rates and sometimes different thermal prehistory of samples are taken into account [19–23]. This is also largely true when comparing PALS experiments with differential scanning calorimetry (DSC) under proper consideration of different heating rates and the different ways of estimating T_g as midpoint of the transition range. Good correlations between T_g values obtained from PALS and DSC have been observed, for example, for amorphous polymers like polystyrene [21,23–27], polycarbonate [21,28], and poly-(vinyl acetate) [22,29]. Frequently, T_gs from PALS are smaller that the values from DSC [23,25,30].

* Corresponding author. Address: ITA Institut für innovative Technologien GmbH, Köthen, Aussenstelle Halle, Wiesenring 4, Lieskau (bei Halle/S), D-06120 Germany. Tel.: +49-345-5512902/8050-950; fax: +49-40-360-3241-463.
E-mail address: gdlubek@aol.com (G. Dlubek).

0032-3861/02/$ - see front matter
PII: S0032-3861(02)00663-8

Table 1
Properties of polymers under investigation. Shown are type and content of comonomer, the density ρ, the glass transition, T_g, from DMA and DSC, and melting (peak) temperatures, T_m, and the crystallinity X_c (assuming $\Delta H_m = 290$ J/g for PE crystals)

Polymer	Content 1-O (wt%)	Density ρ (g/cm^3)	T_g max. E'' (K)	T_g tan δ (K)	T_g DSC (K)	T_m DSC (°C)	X_c DSC (%)
	±0.5	±0.002	±3	±5	±3	±5	±2
HDPE	0	0.963	N.d.	N.d.	N.d.	115	70
P(E-*co*-O07)	7	0.935	244	347	251[a]	113	42
P(E-*co*-O12)	12	0.918	235	284	238	100	33
P(E-*co*-O18)	18	0.903	224	239	227	83	23
P(E-*co*-O24)	24	0.890	218	228	221	64	13

[a] ± 5 K.

Consolaty et al. [30] observed that the difference between the T_gs estimated from PALS and DSC increased with decreasing molar weight of crosslinked polyurethanes. These authors speculated that PALS show a higher sensitivity for initial movements of short chain segments than DSC.

In some cases, such as in poly(methyl methacrylate) [19,20,29], poly(butadiene) and poly(isobutylene) [31], and in epoxy resins [32], the glass transition as detected by PALS appeared more complex and showed two transition temperatures where the transition at the lower temperature was frequently interpreted as sub or secondary transition. In general, positron annihilation has proved to be a valuable complementary tool in correlating the nature of free volume holes at around the glass transition temperature with the nature of the transition.

In semicrystalline polymers the situation appears to be much more complex due to the presence of crystallites and of amorphous regions of different mobilities. In the case of polyethylene, for example, different conventional techniques have produced T_g values ranging from 188 to 258 K [48,49]. The hole volume vs. T curve obtained from positron annihilation experiments in semicrystalline polymers may show a continuous curvature which makes it difficult to estimate a T_g unambiguously. Sometimes, several characteristic temperatures are determined from intersections of straight lines fitted to limited temperature ranges of the curve in which the selection of the fitting ranges seems to be highly arbitrary. Situations such as this have been observed for polyethylenes [33–43] and other semicrystalline polymers [44–47].

Thus, information about the nature of T_g in semicrystalline polymers remains somewhat illusive from conventional techniques and the reliability of a T_g estimated from PALS remain questionable. The aim of this work is to investigate the potential and limits of PALS for studying the glass transition in semicrystalline polymers, this is achieved via a systematic study of the temperature dependence of the mean size of local free volumes in the range between 115 K and 300–350 K for a series of semicrystalline ethylene/1-octene copolymers (P(E-*co*-O)) with a content of 1-octene comonomer between 7 and 24 wt%. Tailor-made ethylene/α-olefin copolymers are of increasing interest owing to the variety of important properties which may be well controlled by the fraction and length of alkyl branches [50,51]. The crystallinity X_c of our P(E-*co*-O)s, decreased systematically from 42 to 13%. For comparison with P(E-*co*-O), a high-density polyethylene (HDPE) with a crystallinity of $X_c = 70\%$ was investigated.

The samples were characterised by DSC, wide-angle X-ray scattering (WAXS) experiments, and density measurements. From positron annihilation experiments, we estimate the T_g, the local free volume at T_g, and the coefficients of thermal expansion of the hole volume below and above T_g for all of the samples. From a comparison of the hole volume with the specific volume, the number of holes is estimated. Correlations between the PALS results and those from dynamic mechanical analysis (DMA) will be investigated. This study continues our previous works on the free volume properties of polyethylenes of different crystallinity [39,52], of ethylene–vinyl acetate copolymers [53], and propylene–α-olefin copolymers [54,55].

2. Experimental

2.1. Polymers

The samples under investigation are listed in Table 1. The ethylene/1-octene copolymers Affinity FM1570 (P(E-*co*-O07)), Affinity PL1880 (P(E-*co*-O12)), and Affinity VP8770 (P(E-*co*-O18)), and DHS 8501.00 (P(E-*co*-O24)) were produced by INSITE™ technology (INSITE™ is a trademark of Dow Chemical Co.) and supplied by Dow Plastics. The mean molar mass was typically $M_w = 10^5$ g/mol and $M_w/M_n = 2–2.5$. A high-density polyethylene (HDPE) with approximately zero branches per 1000 CH_2 was delivered by BUNA AG. For the PALS investigations plates of 1.5 mm thickness were pressed at 180 °C (5 min at 30 bar), followed by a cooling down to room temperature at a rate of approximately 10 K/min.

2.2. Polymer characterisation

For DSC measurements of a heat flux calorimeter, DSC 820 (Mettler-Toledo), calibrated with indium and zinc was

used. The experiments were performed at a heating rate of 10 K/min. The degree of crystallinity of the P(E-*co*-O)s was calculated from $X_c = \Delta H/\Delta H_0$ where ΔH is the melting enthalpy of a copolymer measured during the first heating cycle, and ΔH_0 is the equilibrium melting enthalpy of a completely crystalline polyethylene taken to be 290 J/g [56]. The glass transition temperature T_g was estimated as the midpoint (half-change) of the corresponding stage in the second heat flow curves according to ISO 11357-2.

The WAXS investigations of P(E-*co*-O)s were carried out using a URD 6 (Freiberger Präzisionsmechanik) diffractometer [57]. Scattering patterns were obtained with Ni-filtered Cu K_α-radiation in reflection mode. The crystallinity X_c was determined from the (integrated) crystalline intensity (110 and 200 reflections), I_c, and the intensity of the amorphous diffraction halo, I_a, via $X_c(\mathrm{WAXS}) = I_c/(I_c + 2.17I_a)$, using the method of Hermans and Weidinger [58,59]. In the analysis, we assumed that the crystal structure of P(E-*co*-O) was orthorhombic like in PE, a possible appearance of a hexagonal mesophase was ignored [57]. Effects due to thermal vibrations, lattice imperfections and wavelength-dependent Compton scattering [60] were assumed to be negligible. Furthermore, we interpreted the data in terms of a simple two-phase model, crystalline core and amorphous phase, and considered a possible third, interfacial disordered phase [61] as part of the amorphous phase.

The density ρ of the polymers at 25 °C was determined by a flotation method [62] using mixtures of methanol and water as the flotation medium. For each of the copolymers, several samples were measured in order to establish that they were free of voids.

2.3. Dynamic mechanical analysis

For the dynamic mechanical measurements, a mechanical spectrometer DMTA 3E (Rheometric Scientific) was used. Experiments were performed in tensile mode at a frequency of 1 cycle/s according to ISO 6721-4. For these investigations, bar shaped samples of about 20 mm × 2 mm ×0.2 mm were cut from compression moulded sheets. The samples were analysed by a dynamic strain amplitude of 0.1% at temperatures between −120 and +120 °C. In this temperature range a constant heating rate of 2 K/min was applied. Results obtained were in the form of storage modulus E', loss modulus E'' and loss factor $\tan\delta = E''/E'$ determined.

2.4. Positron annihilation lifetime spectroscopy

All positron lifetime measurements were carried out using a fast–fast coincidence system [1,2] with a time resolution of 260 ps (full width at half-maximum, FWHM, of a Gaussian resolution function) and a channel width of 50 ps. Two identical samples of 1.5 mm thickness were sandwiched around a 1×10^6 Bq positron source (^{22}Na), which was prepared by evaporating carrier-free ^{22}NaCl solution on a Kapton foil of 8 μm thickness. The time resolution of the apparatus and the source components (365 ps/8%, 2000 ps/0.4%) were estimated from the measurement of a reference sample of pure well annealed aluminium ($\tau = 165$ ps).

The temperature dependent measurements were carried out in a purpose built evacuated sample chamber. The temperature was varied between 100 K and 370 (with an accuracy of ± 1 K) in steps of 6 K. In each spectrum a total of $\sim 10^6$ coincidence counts were collected during the measurement which lasted 100 minutes. For the decomposition of the lifetime spectra $s(t)$ we used the conventional analysis in terms of a weighted sum of discrete exponentials [1,2]

$$s(t) = \sum (I_i/\tau_i)\exp(-t/\tau_i) \qquad \sum I_i = 1, \tag{1}$$

where τ_i denotes the mean (characteristic) lifetime of the positron state i, and I_i is the relative intensity of the corresponding lifetime component. After subtraction of the source components and the background the parameters of the lifetime spectra are obtained from a non-linear least squares fitting of $s(t)$, convoluted with the Gaussian resolution function, to the experimental spectra using the routine LIFSPECFIT [63]. Three exponential components were needed to obtain a good fit with a variance of 1.1–1.2.

3. Results and discussion

3.1. Results from DSC, DMA, WAXS, and density measurements

In Table 1, the melting temperature T_m, the glass transition temperatures T_g, the crystallinity X_c, and the density ρ are shown. X_c (from DSC) decreases with increasing content of 1-octene comonomer with a slope of −2.3% per wt% and disappears (extrapolated) for 27 wt%. For all samples the melting starts at 30–40 °C, while the peak temperature of the melting transition used to define T_m decreases with increasing content of 1-octene from 128 to 64 °C with a slope of −2.66 K per wt%. The step in the heat flow curve at T_g is very small for P(E-*co*-O7), but increases with increasing content of 1-octene comonomer. The T_g decreases almost linearly with increasing 1-octene content of the copolymer. The hexyl branches in P(E-*co*-O) lead to a reduced density of packing of the polymers molecules and due to this to a higher segmental mobility observed as lowering of T_g. They disturb crystallisation of the ethylene backbone and cause reduced crystallinity and lamellae thickness. This leads to a decrease of the melting temperature T_m and of the density ρ [56,64,65].

The results of DMA are displayed in Fig. 1(a–c) as storage modulus E', loss modulus E'', and the loss factor $\tan\delta$. At all temperatures, the storage modulus decreases distinctly as the

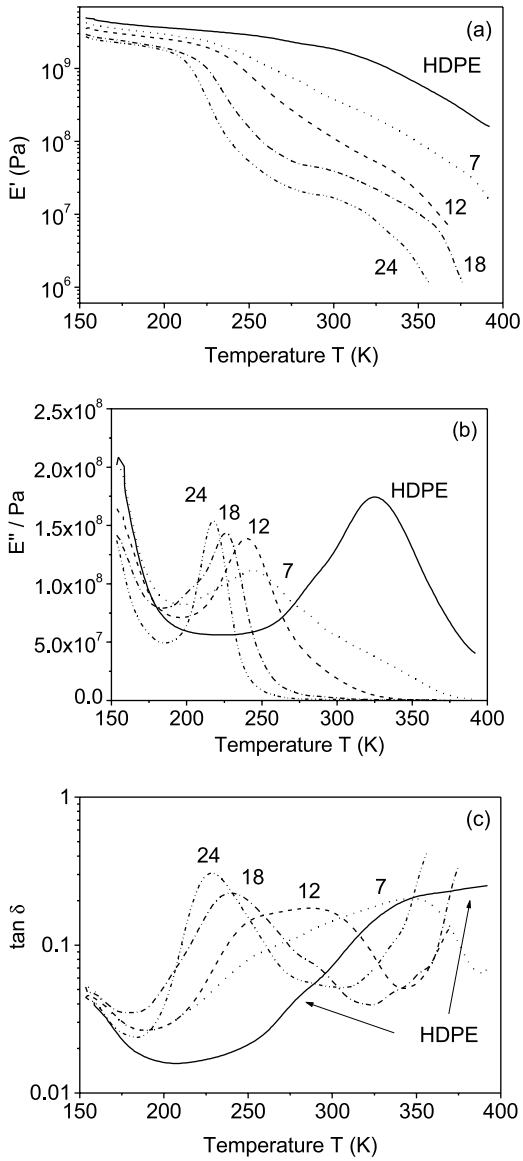

Fig. 1. DMA results for P(E-*co*-O(wt%)) displayed as storage modulus E' (a), loss modulus E'' (b), and the loss factor tan δ (c).

comonomer content increases. In P(E-*co*-O24), E' decreases in two stages, first in the temperature range around 230 K by about two orders of magnitude, and second in the range above 300 K. With decreasing content of 1-octene comonomer these stages shift to higher temperature, show a less pronounced decrease in E', and become more and more smoothed. The decreases in E' around 230 K or somewhat higher temperatures can be considered as softening of the material due to the glass transition, while the decrease at higher temperatures may be due to some other processes including crystal melting.

The loss modulus E'' shows a local maximum at medium temperatures. The peak occurs in P(E-*co*-O24) at 218 K and shows a lowering in intensity and a shift to higher temperature with decreasing content of 1-octene. The peak disappears completely for HDPE and a maximum at 325 K appears which is conventionally attributed to vibrational and reorientational motions within the crystallits [66] (α-relaxation). The loss factor tan δ shows peaks similar to those in E'' but with a much more pronounced shifting and broadening behaviour. The peaks in E'' and tan δ at intermediate temperatures are conventionally labelled as β relaxation and by attributed, by most of the authors, to the (main) glass transition (cooperative segmental motion in the amorphous phase) [67,68]. Some other authors, however, discussed this peak as being associated with motions of chain units in the interfacial region [69].

The glass transition temperature can be determined in principle in three ways: (1) The temperature at which E' has fallen to a certain value or where the inflection point of E' appears; (2) the temperature at which E'' has its maximum value; and (3) the temperature at which tan δ has its maximum value. Commonly, the latter definition is preferred in the literature. As discussed by Boyer [70] and recently in detail by Rieger et al. [71], the definition 3 (and also 1) has some disadvantages, and the best way for defining T_g from DMA is to use the maximum of E''. The physical reason is that E'' is a direct measure of the dissipated energy. In Table 1, the values of T_g estimated from maximum of E'' and from maximum of tan δ are displayed. We will see later, that the determination of T_g from E'' agrees very well with those from PALS while this is not true for the values estimated from tan δ. Apparently, the tan δ behaviour is affected by an interference of the β and α relaxation, which means that, for polymers with higher crystallinity, the peaks corresponding to these relaxations are not separable. As shown in the literature, this interference is particularly strong after quenching of P(E-*co*-O)s [64].

The results of our WAXS studies are shown in Fig. 2 and in Table 2. Despite a broad halo at $2\theta \approx 20°$ attributed to the amorphous phase, two sharp peaks coming from the 100 and 200 interferences of the orthorhombic unit cell are detected. From least squares fitting of a multiple Gaussian function to the scattering profiles, the peak positions and their widths were determined. In case of the highly crystalline linear polyethylene, LPE, the observed reflection angles agree almost with that of undistorted unit cell with the cell parameters [56] $a = 7.4069$ Å, $b = 4.9491$ Å, and $c = 2.5511$ Å, $2\theta_{110} = 21.66°$ and $2\theta_{200} = 24.05°$. θ_{110} and θ_{200} decrease with decreasing crystallinity while the widths of the peaks (not shown) exhibit tendencies to increase. This behaviour indicates the increasing imperfection (paracrystalline distortion, size of crystallites, and lattice defects [72]) of the crystalline phase. Generally, it is assumed that in these copolymers the short-range branches are not incorporated in the crystalline phase [73], however, full exclusion of side chains from the (folded chain) crystal is not completely agreed upon [74].

The crystallinity X_c, derived from WAXS, shows a decrease with increasing content of 1-octene in P(E-*co*-O) which correlates with the DSC results. We take X_c(WAXS)

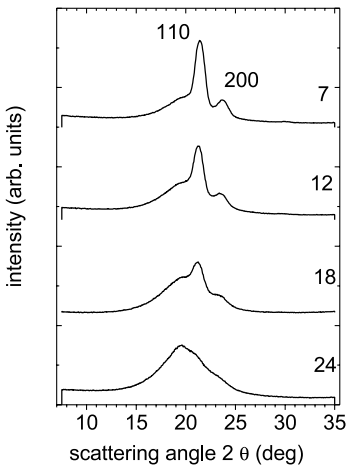

Fig. 2. Wide angle X-ray scattering diagrams of P(E-*co*-O(wt%)).

as mass (core) crystallinity and use this to calculate the specific volume of the (entire, see below) amorphous phase, V_a, from the total specific volume $V = 1/\rho$ via [56]

$$V_a = (V - X_c V_c)/(1 - X_c). \quad (2)$$

In these calculations, we assumed that, due to increasing lattice distortions, the specific volume of the real ethylene crystals, $V_c(X_c)$, increases with increasing content of 1-octene comonomer (decreasing crystallinity) as indicated by the decreasing peak position of the 110 interference. $V_c(X_c)$ was calculated from $V_c(X_c) = [\theta_{110}/\theta_{110}(X_c)]^2 \times V_{pc}$ where $\theta_{110} = 21.66°$ assumed for perfect PE crystals. Furthermore, we assumed that for perfect PE crystals $V_{pc} = 1.000\ cm^3/g$ [56]. The results of this calculation are shown in Table 3 as amorphous density, $\rho_a = 1/V_a$. We found that the density ρ_a of the P(E-*co*-O)s is in the range between $\rho_a = 0.88$ and $0.90\ cm^3/g$ and smaller than the value estimated for HDPE, $\rho_a = 0.92\ cm^3/g$.

3.2. Positron annihilation lifetime spectroscopy

In molecular materials positrons annihilate either as free positrons or from a bound state called positronium (Ps) [2]. The Ps appears either as a *para*-positronium (*p*-Ps, singlet *spin* state) or as a *ortho*-positronium (*o*-Ps, triplet spin state) with a relative formation probability of 1:3. The three lifetime components decomposed from the lifetime spectra

Table 2
Results of WAXS studies. Shown are the crystallinity X_c (see text) and the scattering angles

Polymer	X_c (%)	$2\theta_{110}$ (°)	$2\theta_{200}$ (°)	2θ Halo (°)
	±2	±0.02	±0.05	±0.5
LPE	82	21.61	24.04	20.5
HDPE	70	21.48	23.92	20.6
P(E-*co*-O07)	38	21.43	23.78	20.0
P(E-*co*-O12)	24	21.27	23.65	19.9
P(E-*co*-aO18)	16	21.20	23.6	20.0
P(E-*co*-O24)	7	n.d.	n.d.	19.9

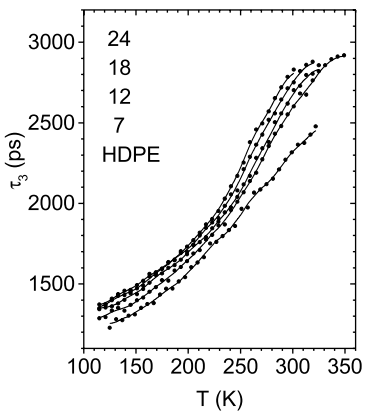

Fig. 3. The temperature dependence of the *o*-Ps lifetime τ_3 of P(E-*co*-O(wt%)) and HDPE.

are consequently attributed to annihilation of *p*-Ps ($\tau_1 \sim 165$ ps), free (not Ps) positrons ($\tau_2 \sim 300$–400 ps), and *o*-Ps ($\tau_3 = 1200$–3200 ps). The values of the lifetime and the intensity of the *o*-Ps, τ_3 and I_3, are sensitive to the properties of the matter in which it annihilates [1–11]. In vacuum, an *o*-Ps has a relatively long lifetime of 142 ns. In matter, during collisions with molecules, the positron of the Ps may annihilate with an electron other than its bound partner and with opposite spin (pick-off annihilation) [2]. The result is a sharply reduced *o*-Ps lifetime depending on the frequency of collisions. In the presence of a sufficient concentration of local free volumes in the sample, the Ps is trapped by these holes and their size controls the *o*-Ps pick-off lifetimes τ_{po} in the ns-range [4–11].

The behaviour of the *o*-Ps lifetime, τ_3 is shown in Fig. 3 for P(E-*co*-O) together with the corresponding values for HDPE. It varies from a minimum of approximately 1200 ps at 100 K to a maximum 2900 ps at 370 K. At room temperature, the *o*-Ps lifetime increases from 2600 ps for P(E-*co*-O07) to 2830 ps for P(E-*co*-O24). These values are distinctly larger than that of HDPE, $\tau_3 = 2320$ ps. This increase mirrors the increasing dimensions of holes at which *o*-Ps is localised and annihilated. A simple model incorporating quantum mechanical and empirical arguments yields an analytical expression relating the hole (assumed spherical) radius (r_h) to the observed *o*-Ps pick-off lifetime [5–8] $\tau_3 = \tau_{po}$

$$\tau_{po} = 0.5\ ns\left[1 - \frac{r_h}{r_h + \delta r} + \frac{1}{2\pi}\sin\left(\frac{2\pi r_h}{r_h + \delta r}\right)\right]^{-1}. \quad (3)$$

The factor of 0.5 ns is the inverse of the spin-averaged Ps annihilation rate, δr represents the extent of the penetration of the Ps-wavefunction into the walls of the hole. The potential of the hole experienced by the Ps may be approximated by a square well potential of finite depth and radius r_h. Since the depth of the potential is unknown it is modelled by a square well potential of infinite depth and radius $r_h + \delta r$ (Tao [5]). $\delta r = 1.66$ Å is obtained by fitting Eq. (3) to observed *o*-Ps lifetime of known mean hole radii

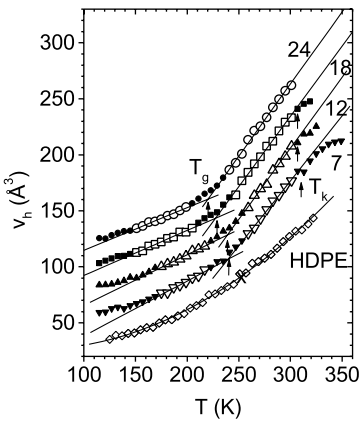

Fig. 4. The temperature dependence of the mean local free volume v_h in P(E-*co*-O(wt%)) and HDPE. For clarity the data are shift on the vertical scale by 20 Å^3 each to the other. The open symbols show the data used for the linear fits. Above the knee temperature T_k the value of v_h does not mirror anymore the true hole size. The data for HDPE are fitted by a second order parabola, the cross indicates the $v_{hg} - T_g$ point obtained by linear extrapolation of the $v_{hg} - T_g$ pairs of P(E-*co*-O). The uncertainties of the experiments are smaller than the size of the data points.

in porous materials [6,7]. Eq. (3) allows the evaluation of an average hole radius r_h and hole volume $v_h = 4\pi r_h^3/3$ from the experimental *o*-Ps lifetime τ_3. The averaging occurs over the size and shape distribution of the local free volumes.

Ortho-Ps may be formed in both the amorphous and the crystalline phase of the semicrystalline polymers. This requires, in principle, a four exponential lifetime analysis involving two *o*-Ps lifetimes. We have performed such analysis in the past for PE [39,52] and its copolymers [53] and for poly(α-olefins) [55]. The results showed, however, that the individual lifetime parameter from a four-component analysis might exhibit a rather large statistical scatter which is due to the high number of fitting parameters and the high correlation among some of them. Due to its dense packing, the Ps yield in the PE crystal is smaller by a factor of about four compared with the amorphous phase [39,52]. Since the highest *o*-Ps lifetime of the three- and four-component analysis differ in our system by a constant value of only approximately 5% [75], we have used, as in Ref. [54], three-component analysis in the current paper.

The hole volume v_h calculated via Eq. (3) and $v_h = 4\pi r_h^3/3$ is shown in Fig. 4. It varies from $v_h = 35$ Å^3 ($r_h = 2.46$ Å) at 100 K to $v_h = 180$ Å^3 ($r_h = 4.24$ Å) at 350 K with a distinct increase in the slope around 230 K in case of the P(E-*co*-O)s. For clarity, we have shifted the curves each to the other by 20 Å^3. At low temperatures, *o*-Ps is trapped in local free volumes within the glassy matrix and τ_3, and hence v_h, show the mean size of static holes. The averaging occurs over the hole sizes and shapes. The slight increase of v_h with temperature mirrors the thermal expansion of free volume in the glass due to the anharmonicity of molecular vibrations and local motions in the vicinity the holes. In the rubbery phase, $T > T_g$, the molecular and segmental motions increase rapidly resulting in a steep rise in the hole size with temperature. Now v_h represents an average value of the local free volumes whose size and shape fluctuate in space and time.

At a higher, critical temperature T_k ('knee' temperature [76]), a tendency of levelling-off of the hole volume expansion can be observed for most of the polymers under investigation. In case of HDPE and P(E-*co*-O24), this deviation may appear at temperatures higher than those investigated. This effect is frequently attributed to the formation of Ps bubbles [2,32], or to the thermal stimulation of various motional and vibrational processes with relaxation times near to or below the *o*-Ps lifetime [15–17,77,78]. Possibly, the PALS knee is the consequence of the disappearance of the dynamic heterogeneity in the glass-forming system at a critical temperature T_c [79]. At that temperature, the mode coupling theory predicts a dramatic change in the dynamics of the liquid [80]. An alternative explanation is the following. The motional processes in the material may excite the *o*-Ps to leave the localised state at a hole and to probe more dense regions of the material. This effect could operate already at relaxations times well below the value of the *o*-Ps lifetime. Thermal detrapping of positrons localised at vacancies in crystals is a well know fact observed for metals at temperatures near the melting point [81,82]. Above the knee temperature T_k, the *o*-Ps lifetime τ_3 and consequently the volume v_h calculated from this do not mirror the true volume of holes [15]. This conclusion we have confirmed by the comparison of PVT and PALS experiments for various polymers, which will be discussed in a subsequent work.

As discussed above, the value of τ_3 and the hole volume, v_h, estimated from this mirror the mean size of free volume holes appearing in the amorphous phase due to the (static or dynamic) disorder. It is known from nuclear magnetic resonance (broad-line ^{1} NMR and high-resolution solid-state ^{13}C NMR), Raman spectroscopy and small-angle X-ray and neutron scattering experiments that semicrystalline polymers, such as PE, can be regarded as having three phases rather than two. These phases, the crystalline, the non-crystalline amorphous and the crystalline-amorphous interfacial phase (see Kitamaru [61] and references given therein) are distinctly different from each other in molecular conformation and mobility. In PE at room temperature, the interfacial phase is essentially amorphous but exhibits only limited molecular motions, while the non-crystalline amorphous phase is rubbery with micro-Brownian segmental motions. Due to the limited resolution of positron experiments, we combine both phases in what we simply call 'amorphous phase'. Due to the different mobilities, both phases are expected to show different size and shape distributions of local free volumes, with a possible transition region between these two phases. Due to this, the hole volume v_h estimated from τ_3 is a mean value, where the averaging occurs over the hole volume and shape distributions in both disordered phases.

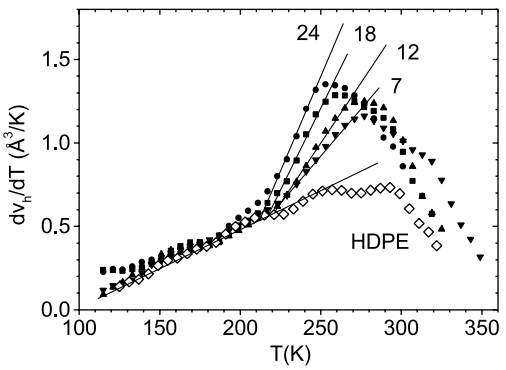

Fig. 5. The differential hole volume dv_h/dT for P(E-*co*-O(wt%)) and HDPE after three-point smoothing.

The increase in the slope of the v_h-T curves for the P(E-*co*-O)s at a temperatures of about 230 K (Figs. 4 and 5) can be related to the glass transition. Since the v_h vs. T dependence is more or less continuously curved in the whole range of temperature,it is not easy to estimated T_g unambiguously. Therefore, we attempted to use the following procedure. First we calculated the differential hole volume, dv_h/dT, from the v_h-T curve. These results are shown in Fig. 5. dv_h/dT shows an increase at low temperatures followed by a strong rise beginning at 200–220 K. The slope of this rise increases with increasing content of 1-octene comonomer. The increase levels-off at temperature of 250–280 K, followed by a decrease. This behaviour mirrors the sigmoidal nature of the $v_h(T)$ curve shown in Fig. 4.

In order to define T_g as the midpoint of the glass transition range as observed via PALS, we approximate the hole volume, v_h, in the surroundings of T_g by the linear relations

$$v_h(T) = v_{hg} + e_{hg}(T - T_g) = v_{hg}[1 + \alpha_{hg}(T - T_g)] \quad \text{for } T < T_g, \tag{4}$$

$$v_h(T) = v_{hg} + e_{hr}(T - T_g) = v_{hg}[1 + \alpha_{hr}(T - T_g) \quad \text{for } T > T_g, \tag{5}$$

Here v_{hg} is the hole volume at $[T_g]e_{hg} = dv_h/dT$ and $\alpha_{hg} = e_{hg}/v_{hg}$, $T < T_g$, denote the expansivity [84] and the coefficient of thermal expansion of the hole volume in the glass phase, $e_{hr} = dv/dT$ and $\alpha_{hr} = e_{hr}/v_{hg}$, $T > T_g$, are the corresponding values for the rubbery polymer.

Fig. 4 shows these fits used for estimating T_g as intersection of two straight lines described by Eqs. (4) and (5). We have fitted the $v_h(T)$ data in the ranges between 150 and 200 K and between 250 and 300 K by straight lines and obtained a first estimate for T_g. In the final analysis we fitted straight lines to the data in the range $T_g - 70\,K \le T \le T_g - 20\,K$ and $T_g + 20\,K \le T \le 305\,K$. The upper temperature limits the fits to the range below the knee temperature T_k. As can be observed from Fig. 4, T_k is always larger than room temperature. The parameters T_g, T_k, v_{hg}, e_{hg}, e_{hr}, $\alpha_{h,g}$, and $\alpha_{h,g}$ estimated from these fits are collected in Table 3.

HDPE is a special case. The differential hole volume, dv_h/dT, shows a continuous increase between 120 and 250 K and an almost constant behaviour between 250 and 300 K. The hole volume itself shows a continuous increase and may be fitted in the whole range of temperature by a second order polynomial function (Fig. 4). Due to the curvature in the v_h vs. T plot, the data may be fitted in limited ranges of temperature by straight lines. Linear fitting of the data in the ranges between 150 and 200 K and 250 and 300 K for example, leads to an intersection point of 210 K. However, this procedure is arbitrary and different intersection points may be obtained by selecting different regions for the linear fits. The ambiguity in T_g reflects the material's dominant crystalline structure whilst the remaining disordered phase shows, due to the constrainment by crystallites, very limited mobility and almost no fraction of freely mobile segments. In this context we remark that the differential hole volume of HDPE, dv_h/dT, agrees below 200 K largely with that of the glassy P(E-*co*-O)s and continues its 'glassy' behaviour at higher temperatures. This implies the absence of a region in HDPE which could be considered as being rubbery in the usual sense (at the appropriate temperature) which is in good agreement with

Table 3
Results of the PALS studies. Shown are the temperatures of the glass transition, T_g, of the minimum in I_3, T_{min}, of the v_h-knee, T_k, the mean local free (hole) volume v_h at T_g (v_{hg}) and at 300 K (v_h), the expansivities, e_{hg} and e_{hr}, and the coefficients of thermal expansion, $\alpha_{h,g}$ and $\alpha_{h,r}$, of hole volume in the glassy and rubbery state (all around T_g), the amorphous density ρ_a, the fractional free (hole) volume at 300 K (f_h) and at T_g(f_{hg}), and the number density of holes N_h

Polymer	T_g (K)	T_{min} (K)	T_k (K)	v_{hg} (Å^3)	e_{hg} (Å^3/K)	$\alpha_{h,g}$ (10^{-3} K^{-1})	e_{hr} (Å^3/K)	$\alpha_{h,g}$ (10^{-3} K^{-1})	$\rho_a^{1)}$ (g/cm^3)	$f_h^{1)}$	f_{hg}	$v_h^{1)}$ (Å^3)	$N_h^{1)}$ (nm^{-3})
	±3	±5	±5	±2	±0.05	±0.3	±0.07	±0.8	±0.005	±0.005	±0.005	±2	±0.05
HDPE	N.d.	~260	>320	N.d.	N.d.	N.d.	N.d.	N.d.	0.919	0.082	N.d.	127	0.64
P(E-*co*-O07)	240	248	310	86.7	0.49	5.7	1.16	13.4	0.899	0.100	0.055	156.5	0.64
P(E-*co*-O12)	239	246	308	88.3	0.45	5.1	1.27	14.4	0.895	0.105	0.056	167.7	0.63
P(E-*co*-O18)	227	238	308	83.3	0.40	4.8	1.25	15.1	0.887	0.113	0.054	173.1	0.65
P(E-*co*-O24)	220	230	>300	80.5	0.38	4.7	1.29	16.0	0.883	0.113	0.050	182.1	0.62

Data for 300 K.

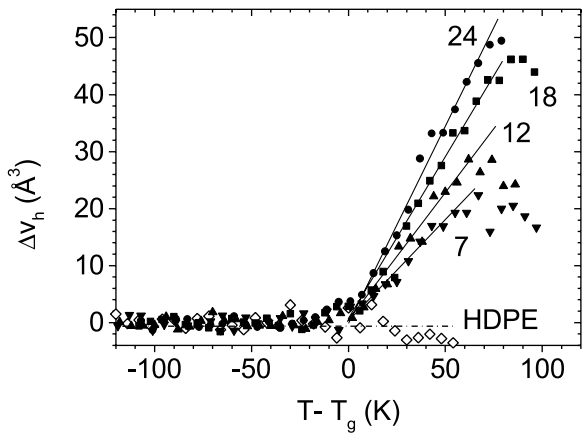

Fig. 6. Difference hole volume $\Delta v_h = v_h - v_{ar}$ as a function of the relative temperature $T - T_g$. v_{ar} was obtained by fitting the v_h vs. T curves below $T_g - 20$ K by a polynomial of second degree (see text).

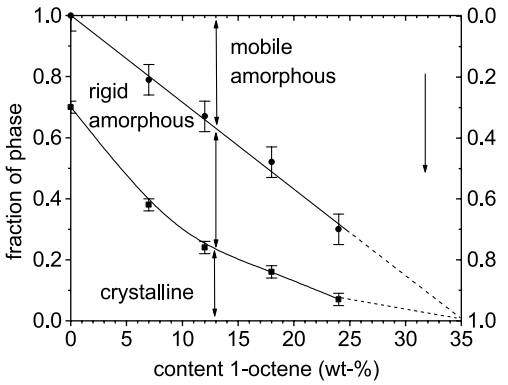

Fig. 7. Mass fractions of the crystalline (X_c, from WAXS), the rigid crystalline–amorphous interfacial (β, from PALS) and the mobile non-crystalline amorphous (γ, from PALS) phases as a function of the content of 1-octene.

the DMA, from which we found that E'' does not show the β relaxation for HDPE.

In this section we attempt to estimate the fractions of the mobile and rigid (immobile) amorphous phases utilising the different thermal expansion behaviour of both disordered phases. When assuming that the thermal expansivity $e_a = e_{hr} = dv_h/dT$ of the mean hole volume (which corresponds to its average over the entire amorphous phase) may be described above T_g by $e_a = e_{am}\gamma^* + e_{ar}\beta^*$, then the (mass) fraction of the mobile amorphous phase, γ^*, can be estimated from

$$\gamma^* = (e_a - e_{ar})/(e_{am} - e_{ar}) = \Delta v_h/\Delta v_h^{max}, \quad (6)$$

where $e_{am} = dv_{am}/dT$ and $e_{ar} = dv_{ar}/dT$ are the thermal expansivities of the hole volume in the mobile (v_{am}) and rigid (v_{ar}) amorphous phases. β^* is the fraction of the rigid phase. The mass fractions β^* and γ^* are given as relative parts of the mass fraction of the amorphous phase, $\alpha = 1 - X_c$, $\gamma^* + \beta^* = 1$. The total mass fraction of the rigid and mobile amorphous phases, β and γ, are given by $\beta = \beta^*\alpha$ and $\gamma = \gamma^*\alpha(\beta + \gamma + X_c = 1)$. In order to get a sufficiently accurate estimate, we initially fitted all the v_h vs. T curves in the temperature range $T < T_g$-20 K to a polynomial of second degree. We assume that this function which describes the thermal expansion of holes in the whole glassy phase, might be extrapolated to the temperature range $T > T_g$ in order to describe the expansion of the rigid amorphous phase (v_{ar}) as we had observed for HDPE. When subtracting this polynomial from the experimental v_h curve we obtain $\Delta v_h = v_h - v_{ar}$. In Fig. 6 we have plotted Δv_h as function of the temperature T shifted by the glass transition temperature T_g, $T - T_g$. In the range between T_g and $T_g + 50$ K, Δv_h increases linearly, the gradient of this section increases with increasing content of 1-olefin and decreasing crystallinity, respectively.

For the actual estimation of γ^* we use this slope and rewrite Eq. (6) as

$$\gamma^* = \frac{[\Delta v_h(T) - \Delta v_h(T_g)]/[T - T_g]}{[\Delta v_h^{max}(T) - \Delta v_h^{max}(T_g)]/[T - T_g]}, \quad (7)$$

where in our case $\Delta v_h^{max}(T_g) = \Delta v_h(T_g) = 0$ and $T = T_g + 50$ K. It is reasonable to assume that for $X_c = 0$, $\gamma^* = \gamma = 1$. Consequently, we estimated the denominator in Eq. (7) from a plot of $[\Delta v_h(T_g + 50\text{ K}) - \Delta v_h(T_g)]/50$ K vs. X_c and obtained at $X_c = 0$ a value of $[\Delta v_h^{max}(T_g + 50\text{ K}) - \Delta v_h^{max}(T_g)/50\text{ K} = 0.816\ Å^3/\text{K}$. We assume that this value is characteristic of the mobile amorphous phase. With these values, β^*, γ^*, β, and γ can be estimated now.

In Fig. 7 we have plotted β, γ, and X_c as function of the content of 1-octene. As can be observed, the crystallinity X_c decreases from 70% for HDPE to zero for P(E-*co*-O) with an content of 1-octene of approximately 35% (extrapolated). The fraction of rigid amorphous phase, β, stays first almost constant at 30–40% and decreases at lower crystallinities. The fraction of the mobile amorphous phase, γ, increases almost linearly with increasing content of 1-octene from 0 for the crystallinity of $X_c = 70\%$ (HDPE) to a value of 1 when X_c disappears. This picture, an antiparallel behaviour of X_c and γ, and an almost constant value of β, seem to be typical. It has been observed in NMR experiments of PE where the crystallinity was varied via variation of the mean molar weight of the polymer [61], and in calorimetric experiments of poly(ethylene terephthalate) where the crystallinity has been varied by changing the temperature and time of crystallisation from the melt [83]. We remark that the estimations done above are based on assumptions the validity of which must be further investigated. Thus, we assumed that the incorporation of 1-octene changes the glass transition temperature, but not directly the slope of the hole expansion in the mobile amorphous phase, e_{am}. The validity of this assumption may be tested by measuring P(E-*co*-O)s copolymers with zero crystallinity but different content of 1-octene. Moreover, we have ignored that the mobile phase

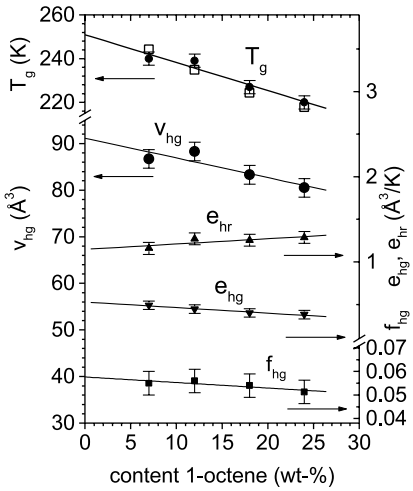

Fig. 8. Glass transition temperature T_g, mean hole volume at T_g, v_{hg}, the expansivity in the rubbery and glassy state, e_{hr} and e_{hg}, and the fractional free volume at T_g, f_{hg}, for P(E-*co*-O) as a function of the content of 1-octene. The lines are due to weight linear least-squares fits through the data from PALS. For T_g: filled circles: PALS; empty squares: DMA.

probably will have a larger weighting than the immobile one in calculating the total expansivity e_a.

In the following paragraph we will discuss the effect of 1-octene comonomers in P(E-*co*-O) on the parameters estimated from the v_h vs. T plots. As shown in Table 3 and in Fig. 8, T_g, v_{hg}, and e_{hg} decrease with increasing content of 1-octene while e_{hr} increases. Linear least-squares fits with constant weight to these data deliver the equations

$$T_g = 251(\pm 4 - 1.275(\pm 0.2)w_O, \quad (8)$$

$$v_{hg} = 91.1(\pm 2.5) - 0.423(\pm 0.15)w_O, \quad (9)$$

$$e_{hg} = 0.529(\pm 0.015) - 0.0065(\pm 0.001)w_O, \quad (10)$$

$$e_{hr} = 1.15(\pm 0.05) + 0.0063(\pm 0.003)w_O, \quad (11)$$

where w_O is the content of octene in wt%, and T_g is given in K, v_{hg} in Å^3, and e_{hg} and e_{hr} in Å^3/K. From these equation, the corresponding parameters of the fits for P(E-*co*-O) with $w_O = 0$, in particularly $T_g = 251$ K, can be read-off. The decrease in T_g with increasing content of 1-octene is easy to understand. The incorporation of hexyl branches weakens the bonding between neighbour chains and leads to a higher segmental mobility and an internal plasticisation of the material shown by the increase in the hole volume v_h at room temperature as well as by the decreases of T_g. We had previously observed similar behaviour for propylene/α-olefin copolymers [54]. Table 3 and Fig. 8 show, that the T_gs from PALS which characterise the glass transition from a microvolumetric point of view agree, within the uncertainties of the experiments, completely with the maxima in E'' attributed to the energy dissipation due to stimulation of the β relaxation (segmental motion), and also with the T_gs estimated from DSC. The value $T_g = 251$ K obtained from extrapolation of the PALS $T_g(w_O)$ to $w_O = 0$ agrees well with maximum of the β relaxation typically observed in branched PE. We notice that the T_gs obtained from the maximum of tan δ do not agree with all of the others, in particular for higher crystallinities.

The hole volume at T_g, v_{hg}, decreases with the content of 1-octene, which may appear surprising. However, several authors have recently observed that for different series' of homo- and copolymers v_{hg} increases linearly with T, $v_{hg} = aT_g$. The slope a was estimated to be $a = 0.33$ Å^3/K [85] and 0.40 Å^3/K [86], respectively. The physical reason for this behaviour is discussed in detail in Ref. [85]. For our data, we obtained from a least-squares fit

$$v_{hg} = 3(\pm 14) + 0.35(\pm 0.06)T_g, \quad (12)$$

where v_{hg} is given in Å^3 and T_g in K. When the straight line is constrained to pass zero during the fit, one obtains $a = 0.366(\pm 0.002)$ Å^3. The value of a corresponds almost to the expansivity in the glassy P(E-*co*-O)s, e_{hg}, which shows that the decrease of v_{hg} is due to the decrease of T_g, and that there is no extra loss or gain in the mean size of the local free volume due to the hexyl branches (see the detailed discussion in one of our previous papers [54,78].

The coefficients of thermal expansion, $\alpha_{h,g}$ and $\alpha_{h,r}$, have values of $\alpha_{hg} \approx 5 \times 10^{-3}$ K^{-1} and $\alpha_{h,r} = (13.4–16) \times 10^{-3}$ K^{-1}. They are larger than the typical coefficients of the specific volume expansion [56,84] by more than one order magnitude. This indicates a fractional free (hole) volume, f_h, of approximately 0.1. As has been discussed previously [39,52–55,62], a more accurate estimate may be obtained in the following way. f_h may be estimated from $f_h = V_f/V_a$, where V_a is the specific volume of the amorphous phase. $V_f = V_a - V_{occ}$ is specific free (hole) volume. The occupied specific volume, V_{occ}, may be approximated by the specific volume of the (perfect) PE crystals, $V_{occ} = V_{cp} = 1.000$ g/cm^3. It represents the most dense packing of the particular polymer consisting of the van der Waals volume and the interstitial free volume. From $V_a = 1/\rho_a$ values of $f_h = 0.100–0.113$ are estimated for P(E-*co*-O)s at a temperature of 300 K (Table 3). With these values of f_h, the number density of holes, N_h, may now be estimated using $N_h = f_h/v_h$. For the P(E-*co*-O)s and HDPE we obtained values of $N_h = 0.62–0.65$ nm^{-3}. Apparently, N_h does not depend on the fractions of the mobile and immobile amorphous phases. The values agree with those estimated previously for PEs of different crystallinity ($N_h = 0.5–0.8$ nm^{-3}) [39,52], for ethylene–vinyl acetate (EVA) copolymers ($N_h = 0.7$ nm^{-3}) [53], and for propylene–α-olefin copolymers ($N_h = 0.6$ nm^{-3}) [54] using the same method. Assuming that N_h does not depend on the temperature, as found previously [19,21,85], we may calculate the fractional free volume at T_g, f_{hg}, from $f_{hg} = N_h v_{hg}$. These values show a slight tendency to decrease with growing w_O and decreasing T_g, respectively (Table 3 and Fig. 8). A distinct increase of f_{hg} with T_g has been observed previously for a larger series of polymers [85].

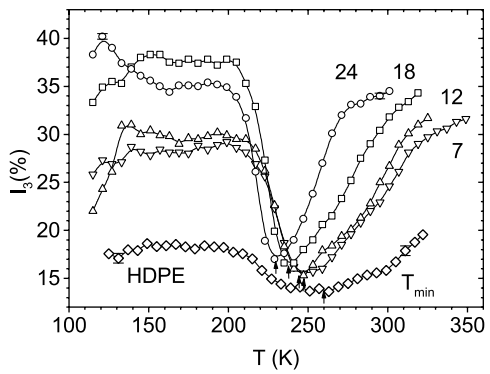

Fig. 9. Temperature dependence of the *o*-Ps intensity I_3 in HDPE and the P(E-*co*-O(wt%))s.

3.3. The ortho-Ps intensity

Fig. 9 shows the temperature dependence of the *o*-Ps intensity I_3. The intensity shows high values between 20 and 40% at temperature below 200 K, a pronounced minimum around 230–260 K, followed by a marked increase above these temperatures. The minimum is most pronounced in copolymers but still exists in HDPE. Such behaviour was already observed for PE by Kindl et al. [33–35] two decades ago. These authors observed also that the value of I_3 at low temperature increases with the length of time the sample is exposed to the positron source. The nature of these effects, however, remained unexplained for a long period.

Recently, the increase of I_3 at low temperature with increasing duration of positron irradiation was explained by the accumulation of secondary electrons shallowly trapped by radicals [29,87]. Thermalisation of the positron injected from the source creates excess electrons and free radicals due to the ionisation. Positrons may combine with shallowly trapped electrons to form Ps. The decrease of I_3 above 200 K was interpreted as a release of weakly bound electrons by the thermal activation of molecules and the recombination of free electrons with reactive species (cations and radicals containing non-saturated bonds). It was also found that irradiation with visible light causes the same effect [40]. Above T_g, concentration of reactive centres will decrease due to the recombination of mobile ions and radicals. This may lead to the new increase of the *o*-Ps intensity above ~250 K. As observed in Table 3, the temperature of the minimum of I_3 varies parallel to T_g with the relation $T_{min} \approx T_g + 10$ K.

4. Conclusion

The *o*-P lifetime detected with PALS mirrors the mean local free (hole) volume v_h appearing in amorphous polymers due to their structural disorder. At the glass transition the disorder changes from a static to a highly dynamic one resulting in a distinct increase of the mean (fluctuating in space and time) hole size with the temperature. This transition may be observed as a discontinuity in the first derivative of the hole volume, dv_h/dT. The discontinuity is expected to be most pronounced in completely amorphous polymers. As observed for the P(E-*co*-O)s, it reduces in semicrystalline polymers with increasing crystallinity. This was attributed to the three-phase character of such material which contains beside the crystalline and the unconstrained (mobile) amorphous phases, a rigid crystalline-amorphous interfacial phase with limited segmental mobility. PALS delivers a mean hole size averaged over the sizes and shapes of holes in both disordered phases.

As long as the discontinuity in dv_h/dT appears, reliable values of T_g may be obtained from PALS via the classical volumetric estimation of T_g from the intersection of two straight lines asymptotically fitted to the free volume expansion curves in the temperature ranges below and above of the expected T_g. The T_gs estimated from PALS data decrease linearly with the weight content of 1-octene comonomer, w_O, between 251 K (extrapolated to $w_O = 0$) and 220 K ($w_O = 24$ wt%). They agree very well with those estimated from DMA (loss modulus E'') and DSC. However, the T_gs obtained from the maximum of tan δ do not agree with all of the others, in particular for higher crystallinities. It was observed that the hole volume at T_g, v_{hg}, decreases linearly with w_O and even with T_g.

For HDPE, any indication of a glass transition could not be observed. From this it was concluded that the whole amorphous phase in this highly crystalline polymer is immobile. From the variation of the thermal expansivity of the local free volume the fractions of the mobile and immobile amorphous phase are estimated. It was observed that the *o*-Ps intensity I_3 shows a minimum at $T_{min} \approx T_g + 10$ K.

Acknowledgements

The authors acknowledge generous financial support from the EPSRC, UK.

References

[1] Dupasquier A, Mills AP Jr., editors. Positron spectroscopy of solids. Proceedings of the International School of Physics Enrico Fermi, Course CXXV, Varenna 6–16 July 1993. Amsterdam: IOS Press; 1995.
[2] Mogensen OE. Positron annihilation in chemistry. Berlin, Heidelberg: Springer; 1995.
[3] Ito Y, Suzuki T, Kobayashi Y, editors. Radiat Phys Chem 2000;58: 401–795.
[4] Triftshäuser W, Kögel G, Sperr P, editors. Mater Sci Forum 2001; 363–5.
[5] Tao SJ. J Chem Phys 1972;56:5499.
[6] Lightbody D, Sherwood JN, Eldrup M. Chem Phys 1985;93:475.
[7] Nakahishi N, Jean YC. Positron and positronium chemistry. In: Schrader DM, Jean YC, editors. Studies in physical and theoretical chemistry, vol. 57. Amsterdam: Elsevier Science Publication; 1988. p. 159.

[8] Jean YC. Microchem J 1990;42:72.
[9] Jean YC. Positron annihilation. He Y-J, Cao B-S, Jean YC, editors. Mater Sci Forum 1995;59:175–8.
[10] Mogensen OE. Positron annihilation in chemistry. Berlin, Heidelberg: Springer; 1995. p. 563.
[11] Pethrick RA. Progr Polym Sci 1997;22:1.
[12] Cohen MH, Turnbull D. J Chem Phys 1959;31:1164.
[13] Vrentas JS, Duda JL. J Polym Sci: Polym Phys 1977;15:403.
[14] Vrentas JS, Vrentas CM. J Polym Sci: Polym Phys 1992;30:1005.
[15] Bamford D, Dlubek G, Reiche A, Alam MA, Meyer W, Galvosas P, Rittig F. J Chem Phys 2001;115:7269.
[16] Bartoš J, Krištiak J, Šauša O, Bandžuck P, Zrubcová J. Macromol Symp 2000;158:111.
[17] Bartoš J, Šauša O, Blochowitz T, Rössler E. J Phys: Condens Matter 2001;13:11473.
[18] Zoller P, Walsh CJ. Standard pressure–volume–temperature data for polymers. Lancaster, Basel: Technomic Publ Co; 1995.
[19] Schmidt M, Maurer FHJ. Polymer 2000;41:8419.
[20] Schmidt M, Maurer FHJ. Macromolecules 2000;33:3879.
[21] Bohlen J, Kirchheim R. Macromolecules 2001;34:4210.
[22] Kobayashi Y, Zheng W, Meyer EF, McGervey JD, Jamieson AM, Simha R. Macromolecules 1989;22:2303.
[23] Yu Z, Yashi U, McGervey JD, Jamieson AM, Shima R. J Polymer Sci B: Polym Phys 1994;32:2637.
[24] Hagiwara K, Ougizawa T, Inoue T, Hirata K, Kobyashi Y. Radiat Phys Chem 2000;58:525.
[25] Stevens JR, Mao AC. J Appl Phys 1979;41:4273.
[26] Hristov HA, Bolan B, Yee AF, Xie I, Gidley DW. Macromolecules 1996;29:8507.
[27] Ban M, Kyoto M, Uedono A, Kawan T, Tanigawa S. J Polym Sci: Part B: Polym Phys 1996;34:1189.
[28] Kluin JE, Yu Z, Vleeshoouwers S, McGervey JD, Jamieson AM, Simha R, Sommer K. Macromolecules 1993;26:1853.
[29] Wang DL, Hirade T, Maurer FHJ, Eldrup M, Petersen NJ. J Chem Phys 1998;108:4656.
[30] Consolaty G, Kansy J, Pegoraro M, Quasso F, Zanderighi L. Polymer 1998;39:3491.
[31] Bandžuch P, Krištiak J, šauša O, Zrubcova J. Phys Rev B 2000;61: 8784.
[32] Jean YC, Sandreczki TC, Ames DP. J Polym Sci: Part B: Polym Phys 1986;24:1247.
[33] Kindl P, Puff W, Sormann H. Phys Stat Solidi (a) 1980;58:489.
[34] Kindl P, Reiter G. Phys Stat Solidi (a) 1987;104:707.
[35] Reiter G, Kindl P. Phys Stat Solidi (a) 1990;118:161..
[36] Tino T, Krištiak J, Hlouskova Z, šauša O. Eur Polym J 1993;29:95.
[37] Okho Y, Uedono A, Ujihira Y. J Polym Sci: Part B; Polym Phys 1995; 33:1183.
[38] Uedono A, Kawano T, Tanigawa S, Ban M, Kyoto M, Uozimi T. J Polym Sci: Part B; Polym Phys 1996;34:2145.
[39] Dlubek G, Saarinen K, Fretwell HM. J Polym Sci B; Polym Phys 1998;36:1513.
[40] Suzuki T, Ito Y, Kondo K, Hamada E, Ito Y. Radiat Phys Chem 2000; 58:485.
[41] Hsu FH, Choi YJ, Hadley Jr. JH. Radiat Phys Chem 2000;58:473.
[42] Li H-L, Ujihira Y, Shukushima S, Ueono K. Polymer 2000;41:92.
[43] Wang CL, Kobayashi Y, Zheng W, Zhang C. Polymer 2001;42:2359.
[44] Ohko Y, Uedono A, Ujihira Y. J Polym Sci: B; Polym Phys 1995;33: 1183.
[45] Uedono A, Suzuki R, Ohadaira T, Mikado T, Tanigawa S, Ban M, Kyoto S, Uozumo T. J Polym Sci: B; Polym Phys 1995;33:1183.
[46] Wang B, Zhang M, Liu WH, Wang SJ, Ito Y, Suzuki T, Kobayashi Y, editors. Radiat Phys Chem 2000;58:355.
[47] Ito K, Nanaswa A, Liu H-I, Ohkubo T, Ujihara Y, Nomura K, Ito Y, Suzuki T, Kobayashi Y, editors. Radiat Phys Chem 2000;58:313.
[48] Gaur U, Wunderlich B. J Phys Chem 1990;93:4490.
[49] Sperlin LH. Introduction into polymer science, 3rd ed. New York: Wiley; 2001. p. 344.
[50] Mäder D, Heinemann J, Walter Ph, Mülhaupt R. Macromolecules 2000;30:1254.
[51] Suhm J, Schneider MJ, Mülhaupt R. J Polym Sci: Part A 1997;35:735.
[52] Dlubek G, Stejny J, Lüpke Th, Bamford D, Petters K, Hübner Ch, Alam AM, Hill MJ. J Polym Sci: Part B; Polym Phys 2002;40:65.
[53] Dlubek G, Lüpke Th, Stejny J, Alam MA, Arnold M. Macromolecules 2000;33:990.
[54] Dlubek G, Bamford D, Rodriguez-Gonzalez A, Bornemann S, Stejny J, Schade B, Alam MA, Arnold M. J Polym Sci: Part B; Polym Phys 2002;40:434.
[55] Dlubek G, Bamford D, Henschke O, Knorr J, Alam AM, Arnold M, Lüpke Th. Polymer 2001;42:5381.
[56] Mark JE, editor. Physical properties of polymers handbook. Woodbury, New York: AIP Press; 1996. Chapter 29.
[57] Androsch R. Polymer 1999;40:2805.
[58] Hermans PH, Weidinger A. Macromol Chem 1961;24:44.
[59] Hermans PH, Weidinger A. Makromol Chem 1961;50:98.
[60] Ruland W. Acta Crystallogr 1961;14:1180.
[61] Kitamaru R, Advances in polymer science, vol. 137. Berlin: Springer; 1998. p. 42.
[62] Dlubek G, Stejny J, Alam MA. Macromolecules 1998;31:4574.
[63] LIFSPECFIT 5.1. Lifetime spectrum fit version 5.1, Technical University of Helsinki, Laboratory of Physics; 1992.
[64] Chen HY, Chum SP, Hiltner A, Baer E. J Polymer Sci: Part B; Polym Phys 2001;39:1578.
[65] Neway B, Hedenqvist MS, Mathot VBF, Gedde UW. Polymer 2001; 42:5307.
[66] McCrum NG, Read BE, Williams G. Anelastic and dielectric effects in solid polymers. New York: Dover; 1991.
[67] Han J, Gee RH, Boyd RH. Macromolecules 1994;27:7781.
[68] Jin Y, Boyd RH. J Chem Phys 1998;108:9912.
[69] Popli R, Glotin M, Mandelkern L, Benson RS. J Polym Sci: Part B; Polym Phys 1984;22:407.
[70] Boyer RF. In: Mark HF, Bikales NM, editors. Encyclopedia of polymer science and technology, Suppl. vol II. New York: Wiley; 1977. p. 745.
[71] Rieger J. Polymer testing 2001;20:199.
[72] Hosemann R, Hindeleh AM. J Macromol Sci—Phys Chem 1995;B34: 327. and reference given therein.
[73] Bensason S, Minick J, Moet A, Chum S, Hiltner A, Baer E. J Polymer Sci: Part B; Polym Phys 1996;34:1301.
[74] Vonk CG, Pijpers AP. J Polymer Sci: Part B; Polym Phys 1985;23: 2517.
[75] Dlubek G, Saarinen K, Fretwell HM. Nucl Instrum Meth Phys Res B 1998;142:139.
[76] Stevens JR, Chung SH, Horoyski P, Jeffrey KR. J Non-Cryst Solids 1994;172-174:1207.
[77] Bartoš J, Krištiak H, Kanaya T. Phys B, Condens Matter 1997;234-236:435.
[78] Dlubek G, Redmann F, Krause-Rehberg R. J Appl Polym Sci 2002;84: 244.
[79] Donth E-J. The glass transition: relaxation dynamics in liquids and disordered materials. Berlin: Springer; 2001.
[80] Götze W, Sjörgen L. Rep Progr Phys 1992;55:241 and references given therein.
[81] Hautojärvi P, Corbell K. In: Dupasquier A, Mills AP Jr., editors. Positron spectroscopy of solids. Proceedings of the International School of Physics Enrico Fermi, Course CXXV, Varenna 6–16 July 1993. Amsterdam: IOS Press; 1995.
[82] Dlubek G, Brümmer O, Meyendorf N. Appl Phys 1977;13:67.
[83] Alsleben M, Schick C. Thermochim Acta 2000;238:294.
[84] Van Krevelen DW. Properties of polymers. Amsterdam: Elsevier; 1990.
[85] Srithawatpong R, Peng ZL, Olson BG, Jamieson AM, Simha R, McGervey JD, Maier TR, Halasa AF, Ishida H. J Polym Sci: Part B; Polym Phys 1999;37:2754.
[86] Bartosch J. J Colloid Polym Sci 1999;274:14.
[87] Hirade T, Maurer FHJ, Eldrup M. Radiat Phys Chem 2000;58:465.